



Sharif University of Technology

Scientia Iranica

Transactions B: Mechanical Engineering

www.sciencedirect.com

Research note

Numerical simulation of LDL particles mass transport in human carotid artery under steady state conditions

A. Nematollahi^a, E. Shirani^{b,*}, I. Mirzaee^a, M.R. Sadeghi^c

^a Department of Mechanical Engineering, Urmia University of Technology, Urmia, P.O. Box 419-57155, Iran

^b Department of Mechanical Engineering, Isfahan University of Technology, Isfahan, P.O. Box 84156-83111, Iran

^c Department of Biomedical Engineering, University of Isfahan, Isfahan, P.O. Box 81746-73441, Iran

Received 27 October 2011; revised 13 February 2012; accepted 3 March 2012

KEYWORDS

Atherosclerosis;
Mass transfer;
LDL;
Carotid artery;
Non-Newtonian fluid.

Abstract In this study, Lumen Surface Concentration (LSC) of Low Density Lipoprotein (LDL) particles in arteries with a permeable wall and up to 60% stenosis under steady state conditions, for Newtonian and non-Newtonian fluids, has been numerically investigated. The results show the Concentration Polarization (CP) phenomenon. Also, an increase in wall suction velocity (high blood pressure) and a reduction in Wall Shear Stress (WSS) are introduced as factors for an increase in LSC. Maximum LSC are observed for 40% stenosis.

© 2012 Sharif University of Technology. Production and hosting by Elsevier B.V.

Open access under [CC BY license](http://creativecommons.org/licenses/by/4.0/).

1. Introduction

One of the most common arterial diseases is atherosclerosis. Atherosclerosis disease is the hardening of artery walls due to the growth of fatty plaques in medium and large arteries. Because fatty plaques are mainly composed of plasma lipoprotein particles, such as LDL, investigating the phenomenon of the mass transfer of LDL particles in the artery wall is an important subject in diagnosing this disease. Arterial diseases are the main cause of human fatalities in most parts of the world. Many studies show a direct relationship between flow patterns and atherosclerosis tissue.

In general, research activities in this field are classified into three categories: experimental, analytical and numerical methods. Wang et al. [1] studied experimentally the surface concentration of albumin in the carotid artery of a dog, and concluded that, due to CP, surface concentration is more than its bulk value in the flow, and, as wall suction velocity increases, LSC rises. Meng et al. [2] investigated CP and

showed that surface concentration is strongly and inversely dependent on WSS, and that disease develops in regions with low WSS. Shukla et al. [3], Chaturani and Samy [4] and Mistra and Chakravarty [5], considering blood analytically as a non-Newtonian fluid, found that the accumulation of cholesterol on an artery wall increases stenosis severity. Deng and Wang [6] numerically observed that under normal physiological conditions, LSC in a direct vessel is 5%–14% higher than the bulk concentration. LSC is also associated with fluid flow and changes linearly with filtration rate and, inversely, with WSS. These results are consistent with experimental results. Yang and Vafai [7] investigated the effect of blood pressure on LSC and concluded that an increase in blood pressure raises LSC, and is effective in disease development. Sun et al. [8], Olgac et al. [9], Soulis and Giannoglou [10] and Fazli et al. [11] showed that in regions with low WSS, the concentration of LDL particles is high.

Due to stenosis in the arteries and the existence of regions with low shear stress in the recirculation region, blood is treated as a non-Newtonian fluid, and it is necessary to consider the flow with non-Newtonian models. The aim of the present study is to investigate the factors affecting LSC. In this study, the artery wall is assumed rigid and permeable to plasma. To simulate the vessel wall, a wall-free model (lumen model) is used [12]. The advantages of this model are low computation cost and the achievement of qualitative information for mass transfer in blood lumen. This model is used by researchers to study the transfer of oxygen [13–15], LDL [16–18] and albumin [19].

* Corresponding author. Tel.: +98 3113915205; fax: +98 3113912628.

E-mail address: eshirani@cc.iut.ac.ir (E. Shirani).

Peer review under responsibility of Sharif University of Technology.



Production and hosting by Elsevier

Nomenclature

C_0	Inlet concentration of LDL particles
C	Concentration of LDL particles
C_w	Wall concentration of LDL particles
D	Diffusion coefficient of LDL particles
\mathbf{n}	Direction perpendicular to the boundary
P	Pressure
r	Radial coordinate
R_0	Radius of vessel (3.5 mm)
Re	Mean inlet Reynolds number
Sc	Schmidt number ($Sc = \nu/D$)
\mathbf{U}	Velocity vector
u	Velocity component in x -direction
U_0	Inlet average velocity
v	Velocity component in y -direction
V_w	Wall suction velocity (4×10^{-8} m/s)
w	Velocity component in z -direction

Greeks

ρ	Blood density (1050 kg/m ³)
μ	Blood viscosity (0.0035 kg/ms)
ν	Kinematic viscosity
τ_y	Blood yield stress.

2. Governing equations

The blood flow is assumed laminar, steady, incompressible and fully developed, and the blood fluid is assumed to be homogeneous, both Newtonian and non-Newtonian models are used.

To simulate the flow, continuity and Navier–Stokes equations are used.

$$\nabla \cdot \mathbf{u} = 0, \quad (1)$$

$$\rho(\mathbf{u} \cdot \nabla)\mathbf{u} = -\nabla P + \nabla \cdot (\mu \nabla \mathbf{u}). \quad (2)$$

In the case of the non-Newtonian model, the modified Casson model is used [20].

$$\mu = \left(\sqrt{\frac{\tau_y(1 - e^{-m\dot{\gamma}})}{\dot{\gamma}} + \sqrt{\mu_c}} \right)^2, \quad (3)$$

where, $\mu_c = 0.0035$ kg/ms, $m = 100$ s and $\tau_y = 0.01$ Pa for a hematocrit of 45% [21].

$\dot{\gamma}$ is shear strain rate and is defined as follows:

$$\dot{\gamma} = \left[2 \left\{ \left(\frac{\partial u}{\partial x} \right)^2 + \left(\frac{\partial v}{\partial y} \right)^2 + \left(\frac{\partial w}{\partial z} \right)^2 \right\} + \left(\frac{\partial u}{\partial y} + \frac{\partial v}{\partial x} \right)^2 + \left(\frac{\partial u}{\partial z} + \frac{\partial w}{\partial x} \right)^2 + \left(\frac{\partial v}{\partial z} + \frac{\partial w}{\partial y} \right)^2 \right]^{\frac{1}{2}}. \quad (4)$$

The mass transfer equation of LDL particles is described as follows:

$$\mathbf{u} \cdot \nabla C = D \nabla^2 C. \quad (5)$$

Because the size of LDL particles are variable, diffusion coefficient is in the range of 5×10^{-12} m²/s to 2×10^{-11} m²/s, and the Schmidt number, Sc , is in the range of 1.6×10^5 to 6.6×10^5 [16,22].

Table 1: Constant coefficient for stenosis severity.

Stenosis severity	30%	40%	50%	60%
λ	0.163	0.225	0.292	0.368

3. Geometry and boundary conditions

The artery is assumed an axisymmetric cylinder, with and without stenosis. The vessel wall is impermeable to LDL particles, and plasma with constant filtration velocity passes through it. Its dimensions are based on characteristics of the carotid artery, the diameter and length are 7 mm and 15.4 cm, respectively, and the distance of 2.8 cm from the beginning of artery is the stenosis region [16]. The geometry of the stenosis is described by the following bell-shaped Gaussian distribution profile [23].

$$R(x) = 1 - \lambda e^{-5x^2} \begin{cases} 0.163 \leq \lambda \leq 0.368 \\ |x| \leq 4. \end{cases} \quad (6)$$

The value of λ depends on the stenosis severity (see Table 1).

Boundary conditions for Navier–Stokes equations are as follows:

At the inlet, a fully developed velocity profile is used. The average velocity (U_0), based on the average flow rate, 275 ml/min, is equal to 0.119 m/s, and the Reynolds number, Re , is 250.

$$u(0, r) = 2 \times U_0 \left(1 - \left(\frac{r}{R_0} \right)^2 \right). \quad (7)$$

At the outlet, the static gage pressure is set to zero. On the wall, the no slip condition and the radial filtration velocity are applied.

$$u(x, R_0) = 0, \quad (8)$$

$$v(x, R_0) = V_w. \quad (9)$$

Boundary conditions for concentration of LDL at the inlet, outlet and wall, sequentially, are as follows:

$$C(0, y) = C_0, \quad (10)$$

$$\left(\frac{\partial c}{\partial x} \right)_{(l,y)} = 0, \quad (11)$$

$$D \left(\frac{\partial c}{\partial \mathbf{n}} \right)_{(x,R_0)} = C_w V_w. \quad (12)$$

4. Numerical method

The structured grid is generated by Gambit software. To investigate the independency of the mesh, LDL concentration profiles along the wall and in the radial direction, at a section near the end of a simple artery (without stenosis), are considered for five different meshes with 18 900, 24 750, 31 500, 36 900 and 43 200 cells, and it is shown that 36 900 cells are adequate. For the artery with 60% stenosis, LDL concentration profiles in the stenosis region and in the radial direction for the number of meshes 52 800, 62 400, 74 880, 86 400, 96 000, and 105 600 are considered, and 96 000 cells have been shown to be adequate for this analysis. The governing equations are solved numerically by Ansys CFX software, using the finite volume and algebraic multigrid methods, based on iteration [24] and coupling pressure and velocity [25]. The convergence criterion for all equations is 10^{-6} , and they are solved using double precision.

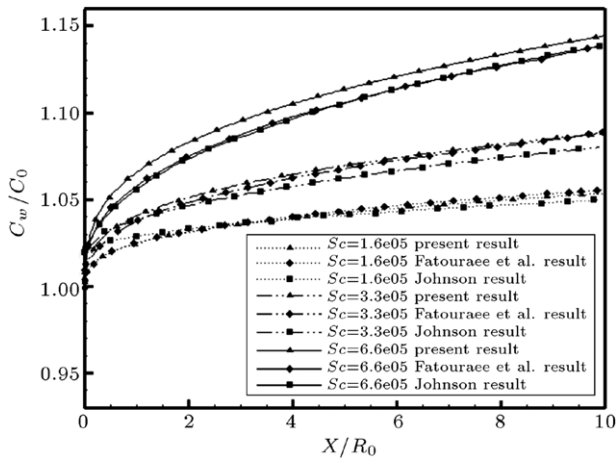


Figure 1: LSC for simple artery and Newtonian fluid.

5. Results and discussion

Numerical simulation of the mass transfer of LDL particles in arteries with and without stenosis, with a lumen model and with a filtration velocity of 10^{-8} m/s on the artery wall, under carotid artery steady flow, has been carried out. It should be noted that Sc is calculated based on the constant viscosity and the diffusion coefficient.

5.1. Concentration polarization (CP) phenomenon

Due to the existence of a filtration rate on the wall, and not passing through the endothelial, LDL particles accumulate on the artery wall, creating a very thin concentration boundary layer. This phenomenon is known as CP. In order to validate the numerical solution, LSC for the Newtonian fluid and the simple artery for various Sc, is given in Figure 1. These results have been compared with the analytical solution of Johnson et al. [26] and the numerical solution of Fatourae et al. [16], and they are in good agreement. The results indicate higher LSC's at the end of the vessel compared to the concentration in the bulk flow for Sc of 1.6×10^5 , 3.3×10^5 and 6.6×10^5 by 8.6%, 14.3% and 23.7%, respectively.

5.2. Effect of WSS on LSC

WSS is an important hemodynamic parameter and is an effective factor in the formation of atherosclerosis [27]. To investigate the correlation between WSS and LSC, Newtonian fluid flow in a simple vessel, with eight flow rates, is taken into consideration. Figure 2 shows that LSC decreased sharply at a low wall shear rate and, by increasing the inlet velocity and, consequently, increasing WSS, LSC decreases and then approaches a constant value asymptotically which is in agreement with results obtained by Ethier [28] and Deng and Wang [6]. As shown in regions where WSS is low, LSC is more sensitive to changes in the flow field.

5.3. Effect of filtration rate and blood pressure on LSC

By increasing the filtration velocity, the LSC of LDL particles, which cannot cross the vessel wall, is increased. From a medical point of view, high blood pressure is an important risk factor in the formation of atherosclerosis disease. The linear relationship

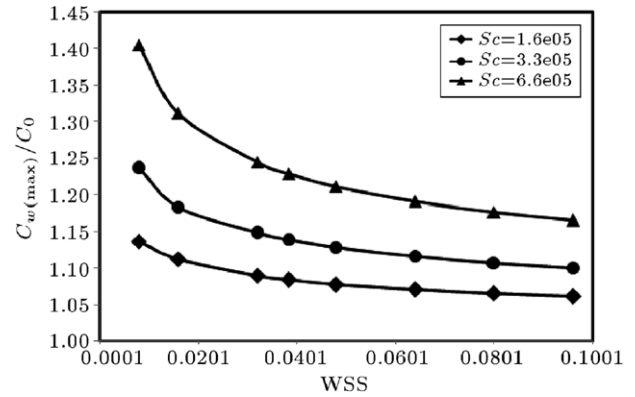


Figure 2: LSC in terms of WSS for a simple artery and in the end of artery.

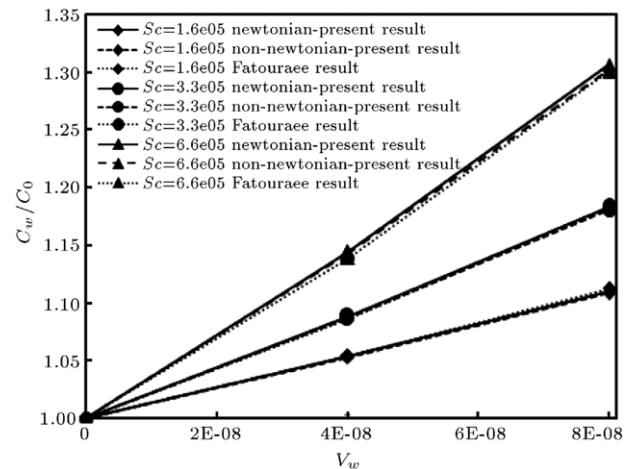


Figure 3: Effect of filtration velocity on LSC in a simple vessel.

between filtration rate and blood pressure is expressed by Poiseuille's equation. To investigate the phenomenon of high blood pressure, a filtration velocity of 4×10^{-8} m/s, which corresponds to a blood pressure of 100 mmHg, and 8×10^{-8} m/s corresponding to 200 mmHg are used [1]. The filtration velocity 4×10^{-8} m/s belongs to normal blood pressure [29]. In Figure 3, the effect of filtration velocity on LSC for Newtonian fluid is shown. Also, these results have been compared with the numerical solution of Fatourae et al. [16] and they are in very good agreement. The results suggest that by increasing the filtration rate, LSC increases linearly, and this is consistent with findings by Deng et al. [30], Deng and Wang [6] and Fazli et al. [11].

5.4. Effect of stenosis severity on LSC

Since accumulation of particles on the vessel wall is the primary cause of disease, in recent years, researchers have studied the transport of materials and the interaction of particles in the recirculation region [31]. In this region, LSC is increased and, therefore, is susceptible to disease progression. Figures 4–7 show WSS and LSC for Newtonian and non-Newtonian fluids for $Sc = 6.6 \times 10^5$. The results suggest that changes in LSC are well correlated with changes in WSS. It can be seen that for 30% stenosis, there is no separation ($WSS > 0$), and for non-Newtonian fluid, LSC is lower than that of Newtonian fluid, which is due to the difference in

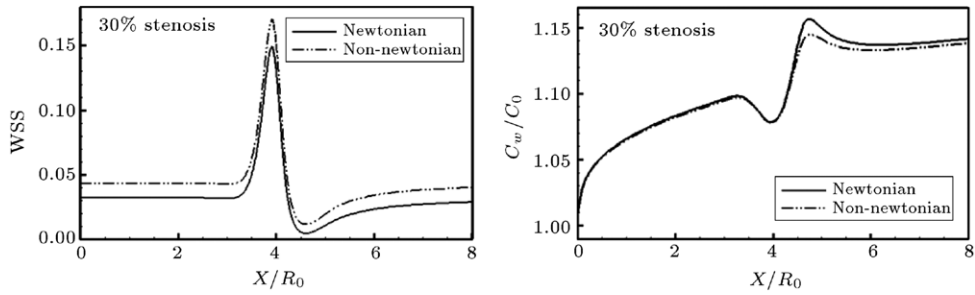


Figure 4: WSS and LSC for 30% stenosis.

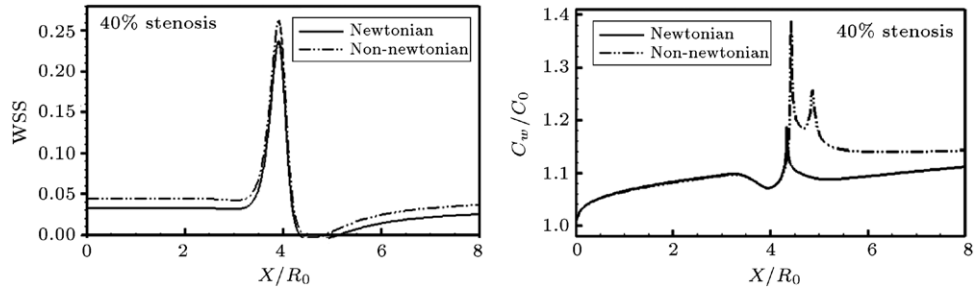


Figure 5: WSS and LSC for 40% stenosis.

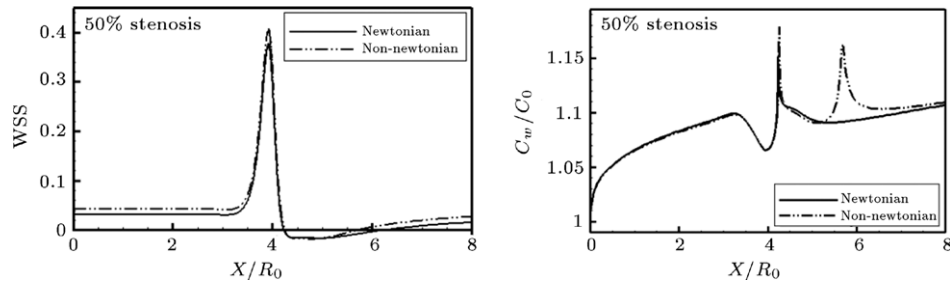


Figure 6: WSS and LSC for 50% stenosis.

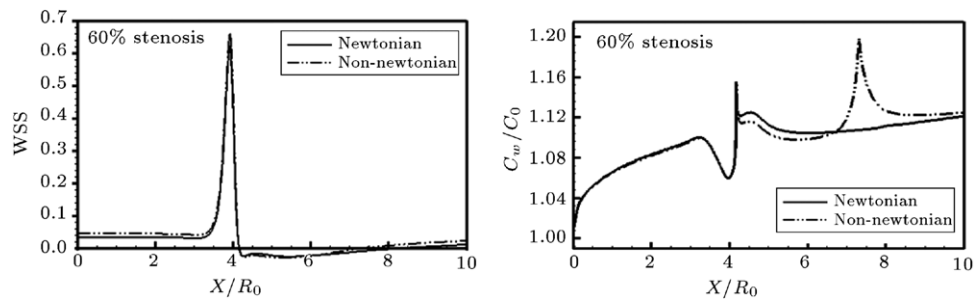


Figure 7: WSS and LSC for 60% stenosis.

velocity profiles. For 40%–60% stenosis, flow separation occurs, which is evident from WSS curves. Due to the existence of the recirculation region, WSS is negative and its value for Newtonian fluid is more than that of non-Newtonian fluid, because the reverse velocity of non-Newtonian fluid is lower than that of Newtonian fluid. At the separation and reattachment points, where WSS is zero, LSC is higher for non-Newtonian fluid. The reason for the increase in LSC at the reattachment point is that in this point shear rate is zero,

and when the non-Newtonian model is used, viscosity and consequently the SC number strongly increases, as a reduction in the concentration boundary layer thickness will increase LSC. This finding is similar to the experimental observations of cholesterol uptake distribution along the stenosed arteries of dogs reported by Deng et al. [32] who showed that the surface concentration and, consequently, the uptake of the 3H-7-cholesterol in the arterial wall is elevated at the location of the reattachment point. Chen et al. [33] used an in-vitro reverse

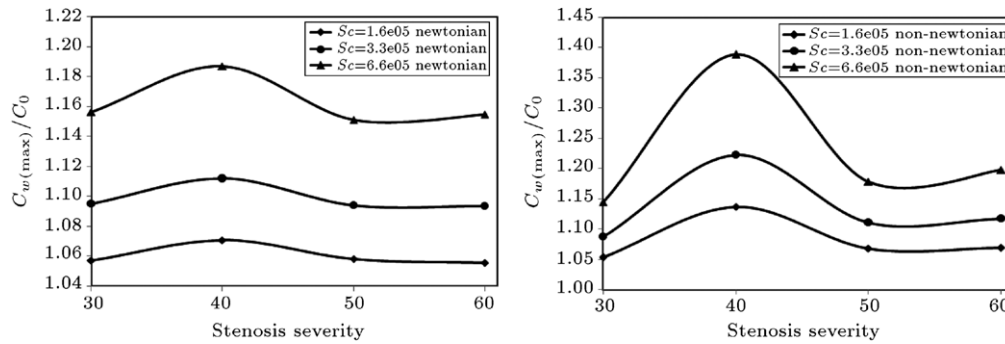


Figure 8: Maximum concentration in the separation region, in terms of stenosis severity for Newtonian and non-Newtonian models.

step model and showed that the particles in blood adhered and transmigrated more in the reattachment region than in the recirculation region. They stated that the reason for this event is the higher concentration of particles in this area.

Research findings suggest that, at separation and reattachment points, where WSS is low, LSC is high, which is an effective factor in the growth of plaque [22,30]. Also, angiography studies show that atherosclerosis plaques grow downstream of stenosis, where reduction in the velocity and instability is shown [34]. Unlike the non-Newtonian model, the Newtonian model (because it has constant viscosity) is unable to demonstrate the increase of LSC at the reattachment point. So, it can be concluded that the non-Newtonian model is more accurate than the Newtonian model. Also, it should be noted that for 40% stenosis, the concentration is highest compared to other stenosis, which is consistent with the findings of other researchers [11,35].

Figure 8 shows the maximum concentration changes in the separation region, with an increase in stenosis severity. The results show that the maximum LSC increases first, with an increase in the severity of stenosis, and then it tends to decrease. So, when stenosis starts, at first, it grows rapidly and then slowly goes forward, narrowing the section of the vessel.

6. Conclusion

The mass transfer of LDL particles in the carotid artery is numerically simulated, with symmetric 30%–60% stenosis, and without stenosis by the lumen model with a filtration velocity of the order 10^{-8} m/s under steady state flow. The results of the numerical solution show that, due to the occurrence of CP phenomena, in the Newtonian fluid, LSC is 8.6%–23.7% higher than that of the bulk flow. With increase in filtration rate (high blood pressure), LSC increase from 8% to 23%. By increasing stenosis severity, the recirculation region becomes larger, and the length of the recirculation region for non-Newtonian fluid is less than that of Newtonian fluid. As WSS increases, LSC decreases and then reaches an asymptotic value. Because of the drastic reduction of WSS at the separation and reattachment points, they are susceptible places for disease development. Also, unlike non-Newtonian fluid, Newtonian fluid is unable to demonstrate the increase of LSC at the reattachment point. So, it can be concluded that using a non-Newtonian model produces more accurate results compared with that of a Newtonian model.

Acknowledgment

We thank the Department of Mechanical Engineering at Isfahan University of Technology of Iran for its support.

Conflict of interest

There are no financial and personal relationships with other people or organizations that could inappropriately influence (bias) their work.

References

- [1] Wang, G., Deng, X. and Guidoin, R. "Concentration polarization of macromolecules in canine carotid arteries and its implication for the localization of atherogenesis", *Journal of Biomechanics*, 36, pp. 45–51 (2003).
- [2] Meng, W., Yu, F., Chen, H., Zhang, J., Zhang, E., Dian, K. and Shi, Y. "Concentration polarization of high-density lipoprotein and its relation with shear stress in an in vitro model", *Journal of Biomedicine and Biotechnology*, 2009, pp. 1–9 (2009).
- [3] Shukla, J.B., Parihar, R.S. and Gupta, S.P. "Effects of peripheral layer viscosity on blood flow through the artery with mild stenosis", *Bulletin of Mathematical Biology*, 42, pp. 797–805 (1980).
- [4] Chaturani, P. and Samy, R.P. "A study of non-Newtonian aspects of blood flow through stenosed arteries and its applications in arterial disease", *Biorheology*, 22, pp. 521–531 (1985).
- [5] Mistra, J.C. and Chakravarty, S. "Flow in arteries in the presence of stenosis", *Journal of Biomechanics*, 19, pp. 907–918 (1986).
- [6] Deng, X.Y. and Wang, G. "Concentration polarization of atherogenic lipids in the arterial system", *Science in China (Series C)*, 46, pp. 153–164 (2003).
- [7] Yang, N. and Vafai, K. "Modeling of low density lipoprotein (LDL) transport in the artery—effects of hypertension", *International Journal of Heat and Mass Transfer*, 49, pp. 850–867 (2006).
- [8] Sun, N., Wood, N.B., Hughes, A.D., Thom, S.A.M. and Xu, X.Y. "Effects of transmural pressure and wall shear stress on LDL accumulation in the arterial wall: a numerical study using a multilayered model", *American Journal of Physiology—Heart and Circulatory Physiology*, 292, pp. H31148–H31157 (2007).
- [9] Olgac, U., Kurtcuoglu, V. and Poulidakos, D. "Computational modeling of coupled blood-wall mass transport of LDL: effects of local wall shear stress", *American Journal of Physiology—Heart and Circulatory Physiology*, 294, pp. H909–H919 (2008).
- [10] Soulis, J. and Giannoglou, G. "Influence of oscillating flow on LDL transport and wall shear stress in the normal aortic arch", *The Open Cardiovascular Medicine Journal*, 3, pp. 128–142 (2009).
- [11] Fazli, S., Shirani, E. and Sadeghi, M.R. "Numerical simulation of LDL mass transfer in a common carotid artery under pulsatile flows", *Journal of Biomechanics*, 44, pp. 68–76 (2011).
- [12] Prosi, M., Zunino, P., Perktold, K. and Quarteroni, A. "Mathematical and numerical models for transfer of low-density lipoprotein through the arterial walls: a new methodology for the model set up with applications to the study of disturbed luminal flow", *Journal of Biomechanics*, 38, pp. 903–917 (2005).
- [13] Qiu, Y. and Tarbell, J.M. "Numerical simulation of oxygen mass transfer in a compliant curved tube model of a coronary artery", *Annals of Biomedical Engineering*, 28, pp. 26–38 (2000).
- [14] Kaazempur-Mofrad, M.R. and Ethier, C.R. "Mass transport in an anatomically realistic human right coronary artery", *Annals of Biomedical Engineering*, 29, pp. 121–127 (2001).
- [15] Kaazempur-Mofrad, M.R., Wada, S., Myers, J.G. and Ethier, C.R. "Mass transport and fluid flow in stenotic arteries: axisymmetric and asymmetric models", *International Journal of Heat and Mass Transfer*, 48, pp. 4510–4517 (2005).
- [16] Fatourae, N., Deng, X.Y., De Champlain, A. and Guidoin, R. "Concentration polarization in the arterial system", *Annals of the New York Academy of Sciences*, 858, pp. 137–146 (1998).

- [17] Wada, S., Koujiya, M. and Karino, T. "Theoretical study of the effect of local flow disturbances on the concentration of low density lipoproteins at the luminal surface of end-to-end anastomosed vessels", *Medical & Biological Engineering & Computing*, 40, pp. 576–587 (2002).
- [18] Wada, S. and Karino, T. "Theoretical prediction of low-density lipoproteins concentration at the luminal surface of an artery with a multiple bend", *Annals of Biomedical Engineering*, 30, pp. 778–791 (2002).
- [19] Rappitsch, G. and Perktold, K. "Pulsatile albumin transport in large arteries: a numerical simulation study", *Journal of Biomechanical Engineering*, 118, pp. 511–519 (1996).
- [20] Papanastasiou, T.C. "Flow of materials with yield", *Journal of Rheology*, 31, pp. 385–404 (1987).
- [21] Fung, Y.C., *Biomechanics: Mechanical Properties of Living Tissues*, Springer, New York (1993).
- [22] Back, L.H. "Theoretical investigation of mass transport to arterial walls in various blood flow regions, part 1: flow field and lipoprotein transport, part 2: oxygen transport and its relationship to lipoprotein accumulation", *Mathematical Biosciences*, 27, pp. 231–262 263–285 (1975).
- [23] Liao, W., Lee, T.S. and Low, H.T. "Numerical studies of physiological pulsatile flow through constricted tube", *International Journal of Numerical Methods for Heat and Fluid Flow*, 14, pp. 689–713 (2004).
- [24] Hutchinson, B.R. and Raithby, G.D. "A multigrid method based on the additive correction strategy", *Numerical Heat Transfer*, 9, pp. 511–537 (1986).
- [25] Majumdar, S. "Role of under relaxation in momentum interpolation for calculation of flow with nonstaggered grids", *Numerical Heat Transfer*, 13, pp. 125–132 (1988).
- [26] Johnson, J.S., Dresner, L. and Kraus, K.A., *Hyperfiltration in Principles of Desalination*, 1, pp. 225–230, Academic Press (1966).
- [27] Malek, A.M., Alper, S.L. and Izumo, S. "Hemodynamic shear stress and its role in atherosclerosis", *The Journal of the American Medical Association*, 282, pp. 2035–2042 (1999).
- [28] Ethier, C.R. "Computational modeling of mass transfer and links to atherosclerosis", *Annals of Biomedical Engineering*, 30, pp. 461–471 (2002).
- [29] Kraiss, L.W., Kirkman, T.R., Kohler, T.R., Zierler, B. and Clowes, A.W. "Shear stress regulates smooth muscle proliferation and neointimal thickening in porous polytetrafluoroethylene grafts", *Arteriosclerosis and Thrombosis*, 11, pp. 1844–1852 (1991).
- [30] Deng, X.Y., Marois, Y., How, T., Merhi, Y., King, W.M. and Guidoin, R. "Luminal surface concentration of lipoprotein LDL and its effect on the wall uptake by canine carotid arteries", *Journal of Vascular Surgery*, 21, pp. 135–145 (1995).
- [31] Kleinstreuer, C., Hyun, S., Buchanan, J.R., Longest, P.W., Archie Jr., J.P. and Truskey, G.A. "Hemodynamic parameters and early intimal thickening in branching blood vessels", *Critical Reviews in Biomedical Engineering*, 29(1), pp. 1–64 (2001).
- [32] Deng, X., Marois, Y., King, M. and Guidoin, R. "Uptake of 3H-7-cholesterol along the arterial wall at an area of stenosis", *ASAIO Journal*, 40, pp. 186–191 (1994).
- [33] Chen, C.N., Chang, S.F., Lee, P.L., Chang, K., Chen, L.J., Usami, S., Chien, S. and Chiu, J.J. "Neutrophils, lymphocytes, and monocytes show differential behaviors of transendothelial and subendothelial migrations under coculture with smooth muscle cells and disturbed flow", *Blood*, 107, pp. 1933–1942 (2006).
- [34] Smedby, O. "Do plaques grow upstream or downstream? an angiographic study in the femoral artery", *Arteriosclerosis, Thrombosis, and Vascular Biology*, 17, pp. 912–918 (1997).
- [35] Wang, G.X., Ye, L.Q., Tang, C.J., Wei, D.H., Lei, D.X. and He, X. "Role of LDL concentration polarization in the atherogenesis by numerical simulation and animal experiment", *Cell Biology International*, 32, pp. S1–S67 (2008).

Ali Nematollahi received his B.S. degree from the Islamic Azad University of Khomeini Shahr, Iran, in 2007 and his M.S. degree from Urumia University of Technology, Iran, in 2011, all in Mechanical Engineering. His research interests include biomechanics and fluid dynamics.

Ebrahim Shirani is Professor of Mechanical Engineering at Isfahan University of Technology, Iran. He received his B.S. degree from Sharif University of Technology, Iran, in 1975 and his M.S. and Ph.D. degrees from Stanford University, USA, in 1977 and 1981, respectively, all in Mechanical Engineering. His research interests include computational fluid dynamics, computational micro and nano-fluid dynamics, turbulence and turbulence modeling, modeling and numerical simulation of interfacial flows, turbomachinery and biofluid dynamics. He is the author of 12 books, and has published 50 journal papers and several conference papers.

Iraj Mirzaee is Associate Professor of Mechanical Engineering at Urumia University of Technology, Iran. He received his B.S. degree from Ferdowsi University of Mashhad, Iran, in 1986, his M.S. degree from Isfahan University of Technology, Iran, in 1989, and his Ph.D. degree from Bath University, UK, in 1997, all in Mechanical Engineering. His research interests include: heat transfer, turbulence modeling and computational fluid dynamics. He has published several papers in international journals and conferences in his areas of interest.

Mahmood Reza Sadeghi is a Ph.D. degree student of Mechanical Engineering at Isfahan University of Technology, Iran, where he is currently a faculty member in the Biomedical Engineering Department. He received his B.S. degree from Bahonar University of Kerman, Iran, in 1991, and his M.S. degree from Tarbiat Modares University, Tehran, Iran, in 1995, all in Mechanical Engineering. His research interests include arterial hemodynamics, cardiovascular modeling, arterial mechanics, computational fluid dynamics and heat transfer, turbulence modeling and computer aided design (CAD).